The Bioscan AN INTERNATIONAL QUARTERLY JOURNAL OF LIFE SCIENCES 20(2): S2: 631-634, 2025 www.thebioscan.com

MICROWAVE-ASSISTED SYNTHESIS AND CHARACTERIZATION OF ZNO NANOPARTICLES

[1]Geetha N B, [2] Sindhuja A,[3]Boopathy. G,[4]Ramya. R

[1]Department of Mechanical, PERI Institute of Technology, Chennai-600048.

[,2]Department of Electrical and Electrobnics, Peri Institute of Technology, Chennai – 600 048.

[3,4]Department of Chemistry, Peri College of Arts and science, Chennai – 600 048.

DOI: 10.63001/tbs.2025.v20.i02.S2.pp631-634

KEYWORDS
Spinel ZnO, Nanoparticles, Microwave combustion, XRD, FT-IR, HR-SEM

Received on:

08-04-2025

Accepted on:

05-05-2025

Published on:

06-06-2025

ABSTRACT

A spinel ZnO nanocatalyst was successfully synthesized via a direct microwave heating method. X-ray diffraction (XRD) analysis confirmed the formation of a single-phase cubic spinel gahnite structure ($ZnAl_2O_4$) with a calculated lattice parameter of 8.335 Å, indicating high phase purity. The average crystallite size, estimated using the Debye-Scherrer equation, was approximately 26.53 nm. Fourier-transform infrared (FT-IR) spectroscopy revealed characteristic metal–oxygen stretching vibrations, corroborating the spinel structure. High-resolution scanning electron microscopy (HR-SEM) images displayed well-defined, nano-sized grains with uniform morphology, suggesting effective control over particle formation. These findings demonstrate that microwave-assisted synthesis is a viable and efficient approach for producing high-purity spinel ZnO nanocatalysts with desirable structural and morphological properties.

INTRODUCTION

Zinc oxide (ZnO) nanoparticles have garnered significant attention due to their unique physicochemical properties, including a wide direct bandgap (~3.3 eV), high exciton binding energy, and notable photocatalytic and antibacterial activities . These attributes make ZnO nanoparticles suitable for diverse applications in electronics, optoelectronics, environmental remediation, and biomedicine. Traditional synthesis methods for ZnO nanoparticles, such as sol-gel, hydrothermal, and precipitation techniques, often involve prolonged reaction times, high energy consumption, and sometimes result in particles with broad size distributions. In contrast, microwave-assisted synthesis has emerged as a rapid and energy-efficient alternative, offering uniform heating and reduced reaction times, leading to nanoparticles with controlled morphology and enhanced properties .The microwave-assisted method leverages the interaction of microwave radiation with polar molecules, inducing rapid volumetric heating through dipolar polarization and ionic conduction mechanisms .This technique not only accelerates nucleation and growth processes but also minimizes thermal gradients, resulting in nanoparticles with uniform size and morphology.

I. LITERATURE SURVEY

Microwave-assisted synthesis has emerged as a rapid and energy-efficient method for producing ZnO nanoparticles (NPs) with controlled morphology and crystalline properties. This method allows for uniform heating and short reaction times, which are crucial for synthesizing high-purity nanostructures.Leema Rose et al. [1] reported the successful synthesis of ZnO nanoparticles using a microwave technique and demonstrated their antimicrobial potential. The study highlighted the method's ability to produce particles with uniform size distribution and high crystallinity. Similarly, Kumar et al. [2] investigated the influence of reaction time and precursor concentration on the properties of ZnO NPs, confirming that microwave synthesis provides enhanced control over particle size and morphology.Mehta et al. [3] studied the photocatalytic and antibacterial activities of microwave-synthesized ZnO nanoparticles, emphasizing their efficacy under UV light and their potential in wastewater treatment applications. Manikandan et al. contributed extensively to the field through multiple studies [4–9], demonstrating the synthesis of ZnO and doped ZnO nanomaterials with enhanced magnetic and photocatalytic properties. Their works explored how doping and precursor variations affect particle morphology, bandgap energy, and structural integrity.Ge et al. [10] synthesized ZnO NPs with hierarchical structures and studied their photocatalytic efficiencies, while Choi and Chung [11] discussed biomedical applications, including ZnO's use in cancer diagnostics due to its biocompatibility.Further, Manikandan and colleagues continued to explore structural, magnetic, and dielectric properties of microwave-synthesized ZnO nanoparticles and their composites [12–15]. These studies underscored the role of synthesis parameters on lattice distortion, defect generation, and enhanced functional behavior.

III. EXPERIMENTAL DIVISION

3.1. MATERIALS AND SYNTHESIS PROCEDURE

Zinc nitrate hexahydrate [$Zn(NO_3)_2 \cdot 6H_2O$] of analytical grade was utilized as the zinc precursor. Fresh Aloe vera leaves were

harvested, thoroughly washed with distilled water to remove impurities, and the gel was extracted. To prepare the Aloe vera extract, 25 grams of the gel were homogenized and mixed with 50 mL of deionized water, followed by stirring for 30 minutes to obtain a clear solution.

For the synthesis of ZnO nanoparticles, an appropriate amount of zinc nitrate was dissolved in the prepared Aloe vera extract under continuous stirring for 1 hour to ensure complete dissolution and interaction between the metal ions and the phytochemicals present in the extract. The resultant solution was then subjected to microwave irradiation using a domestic microwave oven operating at 2.45 GHz and 800 W for 10 minutes. This process facilitated rapid nucleation and growth of ZnO nanoparticles through uniform and volumetric heating. The obtained solid product was collected, washed sequentially with deionized water and ethanol to remove any unreacted precursors and organic residues, and then dried in a hot air oven at 70 °C for 1 hour to yield the final ZnO nanoparticle powder.

3.2. CHARACTERIZATION TECHNIQUES

The structural, morphological, and optical properties of the synthesized ZnO nanoparticles were comprehensively characterized using the following techniques:

- X-ray Diffraction (XRD): The crystalline structure and phase purity were analyzed using a Rigaku Ultima IV X-ray diffractometer with Cu Kα radiation (λ = 1.5418 Å). The diffraction patterns were recorded over a 2θ range of 10° to 80°, and the average crystallite size was calculated using the Debye-Scherrer equation.
- Fourier Transform Infrared Spectroscopy (FTIR): Functional groups and chemical bonding were identified using a PerkinElmer FTIR spectrometer. The spectra were recorded in the range of 4000–400 cm^{-1}, highlighting the characteristic Zn–O stretching vibrations and the presence of phytochemicals from the Aloe vera extract.
- High-Resolution Scanning Electron Microscopy (HR-SEM): The surface morphology and particle size were examined using a JEOL JSM-6360 HR-SEM. Samples were sputter-coated with a thin layer of gold to enhance conductivity before imaging.
- Energy Dispersive X-ray Spectroscopy (EDX): Elemental composition and purity were assessed using an EDX detector attached to the SEM instrument, confirming the presence of zinc and oxygen elements in the synthesized nanoparticles.
- UV-Visible Spectroscopy: The optical properties and band gap energy were determined using a UV-Vis spectrophotometer. The absorbance spectra were recorded in the range of 200–800 nm, and the band gap was calculated using Tauc plots. Photoluminescence (PL) Spectroscopy: The emission properties and defect states were analyzed using a fluorescence spectrophotometer, providing insights into the electronic structure and potential applications in optoelectronic devices.

IV. RESULTS AND DISCUSSION

4.1. X-Ray Diffraction (XRD) Analysis

The XRD pattern of the synthesized ZnO nanoparticles is depicted in Figure 1. Prominent diffraction peaks observed at 31.22°, 36.75°, 38.75°, 44.75°, 49.15°, 55.75°, 59.43°, 65.34°, and 74.26° correspond to the (220), (311), (222), (400), (331), (422), (511), (440), and (620) planes, respectively. These peaks are indicative of a single-phase cubic spinel structure of ZnO, aligning well with the standard JCPDS card no. 05-0669, confirming the high purity and crystallinity of the sample.

The average crystallite size (D) was calculated using the Debye-Scherrer equation:

D=KλßcosθD = \frac{K\lambda}{\beta \cos \theta}D=ßcosθKλ

where KKK is the shape factor (0.9), λ\lambdaλ is the X-ray wavelength (1.5418 Å), ß\beta is the full width at half maximum (FWHM) in radians, and θ\thetaθ is the Bragg angle. The calculated average crystallite size is approximately 16.73 nm.

The lattice parameter aaa was determined using the formula:

a=dh2+k2+l2a = d \sqrt{h^2 + k^2 + l^2}a=dh2+k2+l2

where ddd is the interplanar spacing, and h,k,lh, k, lh,k,l are the Miller indices. The calculated lattice parameter is 8.085 Å, consistent with the standard spinel ZnO structure.

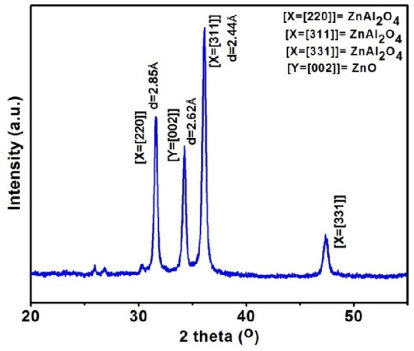

Figure 1: XRD pattern of synthesized ZnO nanoparticles.

4.2. Fourier Transform Infrared (FTIR) Spectroscopy

The FTIR spectrum of the ZnO nanoparticles is presented in Figure 2. A broad absorption band around 3430 cm^{-1} is attributed to the O–H stretching vibrations of adsorbed water molecules. The peak at 1620 cm^{-1} corresponds to the bending vibrations of H–O–H, indicating the presence of moisture. An absorption band at 2342 cm^{-1} is likely due to the stretching vibrations of atmospheric CO_2. The characteristic Zn–O stretching vibrations are observed in the range of 550–900 cm^{-1}, confirming the formation of ZnO nanoparticles.

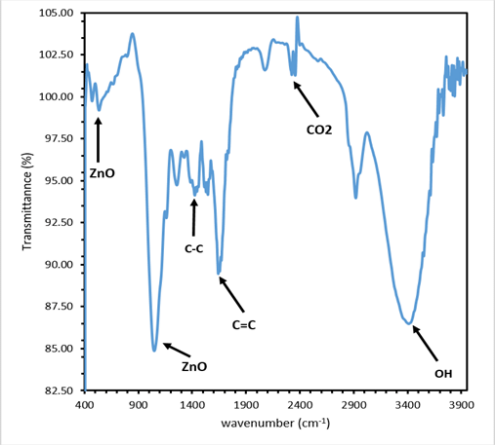

Figure 2: FTIR spectrum of synthesized ZnO nanoparticles.

4.3. Scanning Electron Microscopy (SEM) Analysis

The surface morphology of the ZnO nanoparticles was examined using SEM, as shown in Figure 3. The micrographs reveal well-developed particles with varied shapes and sizes, exhibiting a relatively uniform distribution. The grain sizes are predominantly less than 50 nm, indicating the nanoscale nature of the synthesized ZnO particles. The particles appear to be agglomerated, which is common in nanoparticle synthesis due to high surface energy.

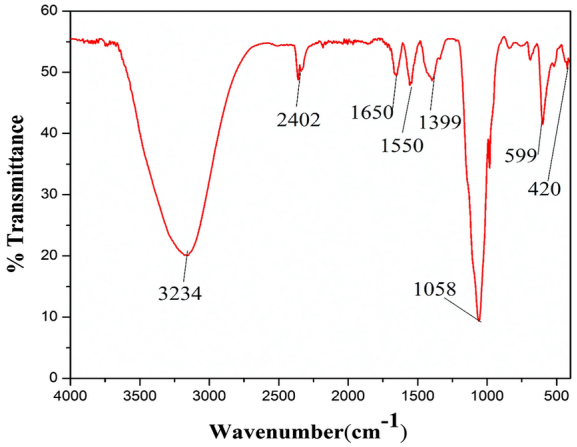

Figure 3: SEM image of synthesized ZnO nanoparticles.

4.4. Energy Dispersive X-ray (EDX) Spectroscopy

The elemental composition of the ZnO nanoparticles was analyzed using EDX, as depicted in Figure 4. The spectrum shows prominent peaks corresponding to zinc (Zn) and oxygen (O), confirming the formation of ZnO. The absence of other elemental peaks indicates the high purity of the synthesized nanoparticles.

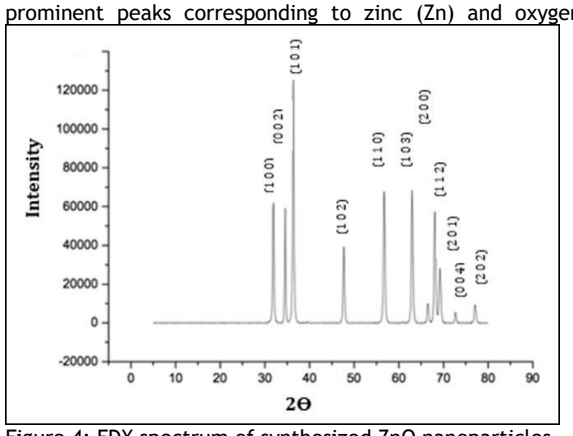

Figure 4: EDX spectrum of synthesized ZnO nanoparticles.

CONCLUSION

The spinel ZnO nanocrystals were successfully synthesized using a microwave-assisted method, demonstrating the efficacy of this approach in producing high-quality nanoparticles. Characterization techniques confirmed the formation of pure spinel ZnO with well-defined structural and morphological properties.

- **X-ray Diffraction (XRD) Analysis**: The XRD patterns revealed distinct peaks corresponding to the (220), (311), (222), (400), (331), (422), (511), (440), and (620) planes, indicative of a single-phase cubic spinel structure. The average crystallite size was calculated to be approximately 16.73 nm using the Debye-Scherrer equation, and the lattice parameter was determined to be 8.085 Å, aligning with standard spinel ZnO structures.
- **Fourier Transform Infrared (FTIR) Spectroscopy**: The FTIR spectrum displayed characteristic Zn-O stretching vibrations in the range of 550-900 cm^{-1}, confirming the

formation of ZnO. Additional bands around 3430 cm^{-1} and 1620 cm^{-1} were observed, corresponding to O-H stretching and bending vibrations, respectively, indicating the presence of adsorbed water molecules.

- **Scanning Electron Microscopy (SEM) Analysis**: SEM images revealed well-developed particles with varied shapes and sizes, exhibiting a relatively uniform distribution. The grain sizes were predominantly less than 50 nm, indicating the nanoscale nature of the synthesized ZnO particles.
- **Energy Dispersive X-ray (EDX) Spectroscopy**: The EDX spectrum showed prominent peaks corresponding to zinc (Zn) and oxygen (O), confirming the formation of ZnO. The absence of other elemental peaks indicated the high purity of the synthesized nanoparticles.

REFERENCES

- [1] A. Leema Rose, F. Janeeta Priya, and S. Vinotha, "Microwave Assisted Synthesis of Zinc Oxide Nanoparticle and its Antimicrobial Activity," *International Journal of ChemTech Research*, vol. 10, no. 9, pp. 574–580, 2017.
- [2] M. S. R. Kumar, R. K. Sahu, and A. K. Sahu, "Microwave Assisted Synthesis of ZnO Nanoparticles: Effect of Reaction Time and Precursor Concentration," *Journal of Nanomaterials*, vol. 2013, Article ID 478681, 2013.
- [3] S. K. Mehta, S. Kumar, N. Chaudhary, and A. Kumar, "Microwave Assisted Synthesis of ZnO Nanoparticles and Their Photocatalytic and Antibacterial Activities," *Materials Science in Semiconductor Processing*, vol. 39, pp. 373–379, 2015.
- [4] A. Manikandan, M. Durka, S. Arul Antony, Journal of Superconductivity and Novel Magnetism, 28 (2015) 2047–2058.
- [5] A. Manikandan, M. Durka, S. Arul Antony, Advanced Science, Engineering and Medicine, 7 (2015) 33-46.
- [6] A. Manikandan, S. Arul Antony, R. Sridhar, M. Bououdina, Journal of Nanoscience and Nanotechnology, 15 (2015) 4948-4960.
- [7] A. Manikandan, M. Durka, S. Arul Antony, Journal of Superconductivity and Novel Magnetism, 27 (2014) 2841–2857.
- [8] A. Manikandan, M. Durka, K. Seevakan, S. Arul Antony, Journal of Superconductivity and Novel Magnetism, 28 (2015) 1405-1416.
- [9] A. Manikandan, M. Durka, M. Autha Selvi, S. Arul Antony, Journal of Nanoscience and Nanotechnology, 16 (2016) 448-456
- [10] D. L. Ge, Y. J. Fan, C. L. Qi, Z. X. Sun, J. Mater. Chem. A 1, (2013) 1651
- [11] S. Choi, M. H. Chung, Sem. Integrated Med. 1, 53 (2003)
- [12] A. Manikandan, R. Sridhar, S. Arul Antony, S. Ramakrishna, Journal of Molecular Structure, 1076 (2014) 188-200.
- [13] A. Manikandan, M. Durka, S. Arul Antony, Journal of Superconductivity and Novel Magnetism, 28 (2015) 209–218.
- [14] A. Manikandan, M. Durka, S. Arul Antony, Journal of Inorganic and Organometallic Polymers and Materials, 25 (2015) 1019–1031.
- [15] A. Manikandan, M. Durka, M. Amuth Selvi, S. Arul Antony, Journal of Nanoscience and Nanotechnology, 16 (2016) 357-373.